Available online at www.sciencedirect.com
SCIENCE DIRECT®
Acta Materialia 52 (2004) 2739–2754
Acta MATERIALIA
www.actamat-journals.com

A combined CALPHAD/first-principles remodeling of the thermodynamics of Al–Sr: unsuspected ground state energies by "rounding up the (un)usual suspects"

Yu Zhong [a,*], C. Wolverton [b], Y. Austin Chang [c], Zi-Kui Liu [a]

[a] *Department of Materials Science and Engineering, The Pennsylvania State University, University Park, 304 Steidle Bldg., State College, PA 16802, USA*
[b] *Ford Research and Advanced Engineering, MD3083/SRL, Dearborn, MI 48121-2053, USA*
[c] *Department of Materials Science and Engineering, University of Wisconsin, Madison, WI 53706-1595, USA*

Received 9 October 2003; received in revised form 6 February 2004; accepted 16 February 2004
Available online 19 March 2004

Abstract

Despite numerous investigations, all previous efforts on thermodynamic modeling of Al–Sr have suffered from inaccurate energetics of either the solid-state compounds or of the liquid alloy. Here, we demonstrate a method yielding simultaneously, accurate solid-state and liquid energetics, as given by first-principles density functional calculations and experimental measurements, respectively. Via first-principles methods, we have investigated the $T = 0$ K energetics of not only the reported ground state compounds in Al–Sr ("the usual suspects"), but also of a wealth of other possible crystal structures observed in isoelectronic alloy systems (somewhat more "unusual suspects"). We find: (i) LDA calculations surprisingly show that Al_2Sr in the $C15$ structure is slightly lower in energy than the observed $CeCu_2$-type structure. However, GGA predicts the opposite order, consistent with the observed $CeCu_2$-type/$C15$ stability. (ii) An as-yet-unreported Al_5Sr_4 compound (observed in Al–Ba) is found to be on the $T = 0$ K ground state hull. (iii) An Al_3Sr_8 phase, isostructural with the recently discovered Al_3Ca_8 compound, is predicted to lie above the ground state hull and is not a $T = 0$ K ground state. Using the first-principles formation enthalpies along with experimental thermodynamic and phase stability information, we have performed a new CALPHAD modeling of Al–Sr, including the three observed intermediate compounds as well as a hypothetical compound Al_3Sr_8. Two different models of the liquid phase were considered: an associate and a random solution model. The descriptions resulting from the two liquid models are critically evaluated with respect to experimental data in the literature and the present first-principles results.

Keywords: Intermetallic compounds; Ab initio electron theory; CALPHAD; First-principles electron theory; Thermodynamics

1. Introduction

Strontium is widely used in industry for the modification of the eutectic microstructure of cast Al–Si alloys. With small additions of Sr, the eutectic structure is converted from a coarse flake structure into a fine fibrous one, often resulting in enhanced mechanical properties [1,2]. Sr is also important as an addition to Mg–Al alloys that enhances the creep resistance of these alloys in high temperature applications [3]. In both cases, the Al–Sr is an important binary subsystem of the multicomponent alloy (Al–Si–Sr and Mg–Al–Sr, respectively), and therefore the thermodynamics of the Al–Sr system is of considerable interest. The phase stability and thermodynamics of the Al–Sr system has been investigated extensively [4–19]. Some of the previous investigations produce accurate thermodynamic properties of the liquid and phase equilibrium, but produce widely varying results for the enthalpies of formation of the solid-state compounds. A recent study has demonstrated that first-principles density functional

* Corresponding author. Tel.: +1-814-863-9957; fax: +1-814-865-2917.
E-mail address: yqz100@psu.edu (Y. Zhong).

1359-6454/$30.00 © 2004 Acta Materialia Inc. Published by Elsevier Ltd. All rights reserved.
doi:10.1016/j.actamat.2004.02.022

calculations [20] provide a means for predicting the solid-state energetics not available from measured data. A simple insertion of these energetics into a CALPHAD description [19] yields good solid-state thermodynamics and an adequate phase diagram, but results in a significant degradation with respect to experiment of the thermodynamics of the liquid phase. In our effort to build an Al–Si–Sr ternary database and a Mg-based alloy database containing Sr, we have returned to the problem of the thermodynamics of Al–Sr. We demonstrate here a method whereby, for the first time, accurate solid-state, liquid, and phase diagram information are all provided by a single, consistent thermodynamic model.

We perform a systematic series of first-principles total energy calculations for the Al–Sr system in both the observed compounds, as well as those observed in a series of A–B systems (A = Al,Ga,In; B = Ca,Sr,Ba) isoelectronic with Al–Sr system. These calculations provide, in some cases, unexpected new insights into the ground state stability of Al–Sr compounds, and is used to consider possible new (as-yet-unreported) Al–Sr phases. The Al–Sr system was remodeled in the present work using a combination of available experimental data in the literature, the present first-principles energetics, and even includes the possible existence of a new finite-temperature stabilized compound Al_3Sr_8. The potential existence of the Al_3Sr_8 compound is predicated on the new compound Al_3Ca_8 discovered recently in the Al–Ca system [21,22].

The Al–Sr system was investigated recently by Wang et al. [23] using the first-principles energetics of the intermetallic phases from [20] and the random solution model for the liquid. In the present work, the thermodynamic properties of the Al–Sr system are investigated using two models for the liquid phase: the random solution model [24] and the associate model [25–27]. Al_4Sr and Al_2Sr were chosen as the associates in the Al–Sr liquid. The resulting thermodynamics and phase diagrams from the two models of the liquid phase were compared with each other and with the available measured data. The thermodynamics and phase diagrams from the associate model are given both with and without inclusion of the Al_3Sr_8 phase.

2. Review of experimental data

Several compilations [5,6,8] exist that collect the Al–Sr binary experimental phase diagram information [16,19]. The phase diagram presented by Chartrand and Pelton [19] included three binary compounds, Al_4Sr, Al_2Sr, and Al_7Sr_8. In the present work, we consider the existence of several new compounds. The crystal structures of these phases along with the observed phases in the Al–Sr binary system are listed in Table 1.

2.1. Thermodynamic data – Al–Sr liquid alloys

The concentration dependence of the enthalpies of mixing of the liquid phase was determined at 1070, 1125, 1130, and 1175 K by Sommer et al. [11] in a high-temperature mixing calorimeter. Their measurements covered two concentration ranges from $x_{Sr} = 0.013$–0.103 and 0.391–0.947. Extrapolation of their measured values indicates a minimum at $x_{Sr} \approx 0.35$ corresponding to $\Delta H = -22.2$ kJ/mol. The measured enthalpies of mixing for the $x_{Sr} = 0.080$ and 0.103 at 1130 K and $x_{Sr} = 0.391$ at 1175 K may not be accurate, as they may lie in the two-phase region. The enthalpies of mixings in the liquid up to 45 at.% at 1773 K were measured by Esin et al. [14] in a high-temperature sealed calorimeter with an isothermal enclosure in an atmosphere of spectroscopically pure helium under an excess pressure of 0.5 atm. The minimum value of the enthalpy of mixing obtained in their study is $\Delta H = -21.3 \pm 0.3$ kJ/mol at $x_{Sr} = 0.35$.

Burylev et al. [5] measured the vapor pressures of strontium over liquid Al–Sr alloys by Knudsen effusion-

Table 1
Partial list of crystal structures of phases considered here in the Al–Sr system

Phase	Pearson symbol	Space group	Strukturbericht designation	Prototype	References
(Al)	*cF*4	$Fm\bar{3}$m	*A*1	Cu	[67]
Al_4Sr	*tI*10	*I*4/*mmm*	$D1_3$	Al_4Ba	[7]
Al_2Sr	*oI*12	*Imma*	–	$CeCu_2$	[7]
Al_2Sr	*cF*24	$Fd\bar{3}$m	*C*15	Cu_2Mg	This work
$Al_{13}Sr_7$	*hP*20	$P\bar{3}$m1	–	$Al_{13}Ba_7$	This work
Al_9Sr_5	*hR*14	$R\bar{3}$m	–	Al_9Sr_5	[68]
Al_5Sr_3	*hP*16	$P6_3/mmc$	–	Al_5Ba_3	This work
Al_5Sr_4	*hP*18	$P6_3/mmc$	–	Al_5Ba_4	This work
Al_7Sr_8	*cP*60	$P2_13$	–	Al_7Sr_8	[69]
Al_3Sr_8	*aP*22	$P\bar{1}$	–	Ca_8In_3	This work
(αSr)	*cF*4	$Fm\bar{3}$m	*A*1	Cu	[67]
(βSr)	*cI*2	$Im\bar{3}$m	*A*2	W	[70]

Note that not all structures given are included in the present modeling (see text for details). References are given for phases observed in the Al–Sr system.

mass loss method between 1123 and 1373 K for two compositions, $x_{Sr} = 0.2$ and 0.33. Vakhobov et al. [6] report the measurements at $x_{Sr} = 0.2$ and 0.5. Despite the apparent difference in composition, these two papers both report the following two relations:

$$\log P_{Sr} = -\frac{12,000}{T} + 8.12 \quad (20 \text{ at.\% Sr } [5,6]), \tag{1}$$

$$\log P_{Sr} = -\frac{12,000}{T} + 9.36 \quad (33.3 \text{ at.\% Sr } [5] \text{ and } 50 \text{ at.\% Sr } [6]). \tag{2}$$

The values of the activities of Sr at 1300 K were given as 0.002 at 20 at.% Sr and 0.03 at 33.3 or 50 at.% Sr separately by Vakhobov et al. [6] and Burylev et al. [5]. Activity data over the entire concentration range were not available until Srikanth and Jacob [17] carried out more complete series of measurements. These authors measured the activities of Sr in the liquid Al–Sr alloys at 1323 K for $x_{Sr} \leqslant 0.17$ using the Knudsen effusion-mass loss technique and for $x_{Sr} \geqslant 0.28$ using the pseudo-isopiestic technique.

2.2. Phase equilibrium data

The Al–Sr system was reviewed by Alcock and Itkin [16] and Chartrand and Pelton [19]. According to their evaluations, the stable phases of the system are the liquid, the Al fcc solid solution, the βSr bcc solid solution, the αSr fcc solid solution, and three intermetallic compounds: Al_4Sr, Al_2Sr, and Al_7Sr_8. (Al_7Sr_8 had been previously described as 'AlSr' or 'Al_2Sr_3' in the literature [7,9,28].)

Burylev et al. [5] and Vakhobov et al. [6,8] investigated the Al–Sr system over the complete concentration range by differential thermal analysis (DTA). Their phase diagrams were characterized by only one intermetallic phase (Al_4Sr), two terminal solutions, and two eutectic reactions between Al_4Sr and the terminal phases. Burylev et al. [5] presented the melting temperature of Al_4Sr as 1273 ± 20 K, and the eutectic reactions in the system as 903 ± 5 K and 3.2 at.% Sr on the Al side and 833 ± 5 K and ~70 at.% Sr on the Sr side.

Bruzzone and Merlo [7] studied the phase diagram by thermal analysis, X-ray diffraction (XRD), and metallographic methods. Al-rich alloys with compositions between 0 and 50 at.% Sr were prepared in sealed iron crucibles, soldered under an argon atmosphere, while Sr-rich alloys were prepared in alumina crucibles under an argon atmosphere. The starting materials were 99.8 wt% pure Sr and 99.999 wt% pure Al. Three compounds were reported: Al_4Sr, Al_2Sr, and 'Al_2Sr_3'. The first melts congruently at 1313 K, and the second and third decompose by peritectic reactions at 1209 and 939 K, respectively. 'Al_2Sr_3' and βSr form a eutectic reaction at 81.75 at.% Sr and 863 K; no information was given about the eutectic reaction between (Al) and Al_4Sr, except a line drawn at 933 K. A compound near Al_7Sr_8 stoichiometry was reported, although AlSr was adopted in the phase diagram, because the precise nature of Al_7Sr_8 was not confirmed at that time due to experimental difficulties. The existence of a possible new phase in the Sr-rich region under 937 K was also postulated. The liquidus of $L + Al_2Sr \Longleftrightarrow Al_2Sr_3$ (Al_7Sr_8) may not be much reliable, because very few liquidus points were detected while many experiments were done in that range.

Vakhobov et al. [9] reexamined the system using purer materials and longer annealing times, produced by combined vacuum distillation and directional crystallization. They confirmed some of the results of the previous investigations [5,6,8]. Particularly, their results agree well with the phase diagram drawn from the results of Bruzzone and Merlo [7]: the eutectic reaction on the Sr side was shown at about 77 at.% Sr and 833 K, the melting point of Al_4Sr coincides with the value of Bruzzone and Merlo [7]; and the peritectic reactions of formation of Al_2Sr and 'Al_2Sr_3' were given as occurring at 1213 and 951 K, respectively.

Hanna and Hellawell [10] studied the Al-rich part of the system up to 2 at.% Sr by thermal analysis. The temperature and composition of the eutectic point were found to be 926 K and 1.3 at.% Sr. Sato et al. [13] studied the Al-rich part of the system up to 7.2 at.% Sr by thermal analysis, XRD, and optical microscopy and found the eutectic at 0.85 at.% Sr and 927 K.

Closset et al. [15] performed an investigation of the Al–Sr diagram with DTA, XRD, and optical microscopy. The samples were melted under an argon atmosphere in an induction furnace. For alloys containing less than 60 wt% Sr (31.5 at.% Sr), alundum crucibles were used; for alloy's composition range between 60 and 90 wt% Sr (31.5–73.5 at.% Sr), alumina crucibles were used; for alloys with more than 90 wt% Sr (73.5 at.% Sr), iron crucibles were used. All crucibles were isolated in low-density refractory insulation to slow down the rate of cooling and to give a uniform cooling. Heating and cooling curves for each sample were measured to confirm the liquidus. Their results confirmed the general features of the diagram by Bruzzone and Merlo [7], but some of the quantitative values are quite different. Closset et al. [15] confirmed the eutectic reaction on Al-rich side (reported at 927 K and 2.4 wt% Sr (0.75 at.% Sr)). The melting point of the Al_4Sr compound was given as 1298 K, the peritectic reactions of the Al_2Sr and 'AlSr' (instead of the 'Al_2Sr_3' in [7]) compounds at 1193 and 937 K, respectively. The eutectic reaction on the Sr side was shown at 853 K and 90 wt% Sr (73.5 at.% Sr). Closset et al. [15] also mentioned their difficulties with detection of thermal arrests in alloys prepared by using iron crucibles. These difficulties may hurt their accuracies of the samples containing more than 90 wt% Sr

(73.5 at.% Sr). In all, it seems that the liquidus of the Sr concentrations lower than 90 wt% (73.5 at.%) are more reliable than those obtained by Bruzzone and Merlo [7], while higher than 90 wt% (73.5 at.%) are less reliable than those by Bruzzone and Merlo [7].

3. First-principles methodology

Because no accurate measurements of the solid-state energetics of Al–Sr compounds exist, we have instead turned to first-principles density-functional-based calculations to supply these energetics. The first-principles calculations described below utilize the plane wave pseudopotential method, as implemented in the highly efficient Vienna ab initio simulation package (VASP) [29–32], using ultrasoft pseudopotentials [33,34]. In many of the calculations reported here, the local density approximation (LDA) was employed, with the exchange-correlation functional of Ceperley and Alder [35,36]. As a test of the accuracy of the energetics, several calculations were performed using different methods and exchange-correlations: the full-potential linearized-augmented planewave (FLAPW) [37,38] and projector-augmented planewave (PAW) methods as well as a generalized gradient approximation (GGA). Tests were performed for Sr treating 4p electrons as valence vs. core, and it was found to be important for quantitatively accurate results to treat 4p electrons as valence. All structures were fully relaxed with respect to volume as well as all cell-internal and -external coordinates. Convergence tests indicated that 162 eV was a sufficient cutoff to achieve highly accurate energy differences (in several tests, these energies were equal to those with significantly higher cutoffs to within 0.1 kJ/mol atoms or 1 meV/atom). Extensive tests of **k**-point sampling using both Monkhorst–Pack [39] **k**-point meshes showed that the meshed used here (typically, from $8 \times 8 \times 8$ to $16 \times 16 \times 16$ grids) indicated that total energy differences were converged to within $\sim$0.1 kJ/mol. Details of the FLAPW calculations have been described previously [20], and the VASP–PAW and VASP–GGA calculations were performed with similar settings as the LDA calculations, with the exception that the PAW calculations used a larger cutoff of 301 eV.

4. The ground state problem: cluster expansions vs. "rounding up the usual suspects"

First-principles calculations are continually gaining acceptance as a useful complement to experimental methods of phase stability determination. However, these methods rely on a crystal structure as input. In other words, in the complete absence of experimental information on a crystal structure, there is, in general, no method by which one can *truly predict* the stable crystal structure from first-principles methods alone. This situation was described in 1988 as "scandalous" [40], and a general solution to this problem has not emerged in the intervening 15 years. What is commonly done in the application of first-principles to crystal structure determination is simply to calculate energetics of all of the structures that are experimentally observed for a given system and then declare the lowest-energy structure(s) the "ground states". Zunger and co-workers [44] have referred to this method as "rounding up the usual suspects", an apt description, since one must *suspect* that a given structure is stable in order to include it in the set of candidates. Thus, by definition, this method is unlikely to provide truly predictive results in the form of new and unexpected ground state structures.

An alternative to "rounding up the usual suspects" which does, in fact, provide a truly predictive method of ground state search *for a limited subset of alloy problems* is the cluster expansion methodology [41–44]. In this method, a lattice type (e.g., fcc, bcc, hcp) is first assumed, and then first-principles energetics of a variety of structures that are all substitutional arrangements of atoms on this lattice type are mapped onto a generalized Ising-like Hamiltonian. This Hamiltonian can subsequently be subjected to analysis by linear programming [45], direct enumeration [43], or Monte Carlo techniques [44] to predict the stable crystal structure out of the astronomical number 2^N for a binary system with N lattice sites) of possible configurations. This technique has been applied with great success to many bulk ordering problems providing predictions, e.g., of new ground states structures in metallic [43,44] and ceramics systems [46,47], short-range order in solid solutions [48,49], phase diagrams [44,50,51] and coherent precipitate GP zone structures [52].

However, the usefulness of this method is severely compromised by the constraint to a single, assumed lattice type. The vast majority of alloy systems (like the Al–Sr system examined here) do not contain ordered compounds that are merely substitutional rearrangements of atoms on a specific lattice type. Even within a single alloy system, the stable crystal structures generally consist of a both complex *topological* as well as substitutional patterns. The cluster expansion methodology cannot be used to predict ground state topologies of crystal structures, and thus we cannot use this method to predict ground states for the Al–Sr system.

5. Searching for ground state crystal structures in Al–Sr: can we learn something truly unexpected by "rounding up the (un)usual suspects"?

We therefore turn to an alternative: rather than simply "rounding up the usual suspects" by examining

Table 2
Crystal structures reported in the A–B systems (A = Al,Ga,In; B = Ca,Sr,Ba), isoelectronic with Al–Sr

System	A_4B	A_2B	"AB"	B-rich
Al–Ca	$D1_3$	$C15$	$Al_{14}Ca_{13}$	Al_3Ca_8
Al–Sr	$D1_3$	$CeCu_2$-type, Al_9Sr_5	Al_7Sr_8	–
Al–Ba	$D1_3$	$Al_{13}Ba_7$, Al_5Ba_3	Al_5Sb_4-type	–
Ga–Ca	"$D1_3$"	In_2Ca-type, $C32$	B_f	$Ga_{11}Ca_{28}$, Ga_3Ca_8, Ga_7Ca_{11}
Ga–Sr	$D1_3$	$C32$	Al_7Sr_8-type	–
Ga–Ba	$D1_3$	$C32$	Al_7Sr_8-type	$Al_{10}V$-type
In–Ca	–	Ga_2Yb-type	$B2$	$D0_3$ ($InCa_3$)
In–Sr	Ni_3Sn-type	Ga_2Yb-type	InSr	$D0_3$ ($InSr_3$), $D8_1$ (In_3Sr_5)
In–Ba	$D1_3$	$CeCu_2$-type	InBa	$InBa_{13}$, $InBa_3$, $InBa_2$

only the observed crystal structures in Al–Sr, we expand our pool of crystal structure "suspects" by considering somewhat unusual structures that are nevertheless suspected to be competitive in energy. To achieve the pool of candidate structures, we consider the observed crystal structures for systems that are isoelectronic with Al–Sr, namely, the nine binary A–B systems, where A = Al,Ga,In and B = Ca,Sr,Ba. These systems possess a rich variety of crystal structure types, but also share some interesting commonalities: All of the systems show strongly ordered intermetallic compounds with high melting points, and almost all have compounds of A_4B and A_2B stoichiometries, a compound near AB stoichiometry as well as one or more B-rich compounds. Table 2 shows the observed crystal structures reported in the nine A–B systems near the A_4B, A_2B AB, and B-rich stoichiometries. Our approach will be to consider the energetics of Al–Sr compounds in the crystal structures shown in Table 2, as well as a few other structures. We note, of course, that although we have enhanced our set of candidate structures, this method still amounts to trying only a handful of ~20 candidate structures. Thus, this cannot be considered a true ground state prediction in the sense that it is possible that even lower-energy structures exist that are missed by the present approach. However, we show here that even this limited search can nonetheless produce some unexpected results in the sense of structures lower in energy than the reported crystal structures as well as reported phases that do not appear on the $T = 0$ K ground state hull. Both these types of observations yield insights into the stabilization of phases in Al–Sr by entropic effects.

6. First-principles results: unexpected energetics in Al–Sr

We have computed the LDA energetics of Al–Sr compounds in most of the structure types of Table 2, as well as a few other common structure types. For the crystal structures yielding low energies in the LDA, we have also computed ΔH using the GGA and GGA–PAW approaches. The comparison of LDA vs. GGA demonstrates the effect of exchange correlation treatment on the energetics in this system, whereas GGA vs. GGA–PAW tests the applicability of the pseudopotential approach. We find very little difference between ultrasoft pseudopotential and PAW calculations, confirming that the pseudopotential approximation is reliable for this system. However, as we show below, there are significant, and even qualitative, differences between the LDA and GGA calculations, and the latter generally seems to give phase stability more consistent with experimental reports. We remind the reader that although calculations are *numerically* converged well within 1 kJ/mol, this quantity is a good rule-of-thumb estimate for the *physical* accuracy of these calculations. In the following discussion, we consider differences between calculated results greater than 1 kJ/mol to be significant.

Table 3 gives the calculated formation enthalpies, ΔH, for all structures considered. All structures are indicated by Struktürbericht designation or prototype with one exception that is denoted SQS-16, a 16-atom "special quasi-random structure" constructed to mimic a hypothetical fcc Al_3Sr solid solution [53]. Fig. 1 shows the ΔH results plotted as a function of composition and the resulting ground state convex hull constructed from these energetics. Many of the qualitative trends of the first-principles results are in agreement with the experimental reports: The calculated energies of the observed structures are all very low, with the hypothetical Al–Sr compounds in the crystal structures of the isoelectronic systems also competitive in energy for many structures. On the other hand, the structures that are not observed in any of the isoelectronic systems (e.g., CaF_2, $L1_2$) are all extremely high in energy, with positive formation enthalpies, in some cases. However, a closer inspection yields some interesting and unexpected results.

6.1. Al_4Sr stoichiometry

The observed Al_4Ba-type structure is low in energy and has a strong, negative ΔH for both LDA and GGA, consistent with the observed high melting point of this compound. The GGA results for $\Delta H(Al_4Sr)$ are more stable (more negative) than LDA. For this stoichiome-

Table 3
First-principles calculated formation enthalpies, ΔH (kJ/mol atoms), for Al–Sr in a variety of ordered structure types

Stoichiometry	Structure	VASPΔH (LDA)	VASP–PAW ΔH (LDA)	FLAPW ΔH (LDA)	VASP ΔH (GGA)	VASP–PAW ΔH (GGA)
Al_4 Sr	**Al_4Ba-type**	**−24.2**	**−23.7**	**−22.8**	**−25.6**	**−26.2**
Al_3Sr	Ni_3Sn-type	−18.4				
Al_3Sr	"SQS-16"	−11.6			−12.3	
	$L1_2$	− 5.5				
Al_2Sr	**$CeCu_2$-type**	**−29.7**	**−27.4**	**−27.9**	**−29.0**	**−28.8**
	*C*15	−30.3	−29.0		−27.4	−27.2
	*C*14	−28.2				
	*C*36	−29.8				
	*C*32	−23.0				
	$CaIn_2$-type	−26.0				
	*C*16	+ 0.5				
	Si_2Sr-type	−9.0				
	$MoPt_2$-type	−8.2				
	CaF_2-type	+ 55.4				
$Al_{13}Sr_7$	$Al_{13}Ba_7$-type	−29.8			−27.8	−27.3
Al_9Sr_5	**Al_9Sr_5**	**−29.4**			**−27.9**	**−27.7**
Al_5Sr_3	Al_5Ba_3-type				−27.5	−27.2
Al_5Sr_4	Al_5Ba_4-type	−26.7			−26.0	−25.6
$Al_{14}Sr_{13}$	$Al_{14}Ca_{13}$-type	−22.4				
AlSr	B_f	− 17.3				
	*B*2	−12.7				
Al_7Sr_8	**Al_7Sr_8**	**−18.9**			**−21.9**	**−21.4**
Al_3Sr_8	Ca_8In_3-type	−10.1			−10.6	−10.1
$AlSr_{10}$	$Al_{10}V$-type	+8.4				

Structures observed in the Al–Sr system are shown in bold.

try, there is no other reported crystal structure observed in any of the isoelectronic systems. There is, though, a Ni_3Sn-type structure in the In–Sr system. The first-principles calculated energy of Al_3Sr in this structure is clearly above the Al_4Sr ground state.

6.2. Al_2Sr stoichiometry

Although the $CeCu_2$-type structure is low in energy, the VASP–LDA calculation surprisingly places this observed structure slightly higher in energy than the *C*15 phase. The *C*15 structure is observed in the Al–Ca system, but not in Al–Sr. In a recent study of Al–Cu [54], a similar situation occurs in that first-principles energetics of the observed Al_2Cu ground state structure (*C*16) are slightly higher in energy than that in the CaF_2-type structure. In the case of Al_2Cu, vibrational entropy was shown to reconcile the $T = 0$ K ground state results with the finite temperature experimental observations. It is possible that vibrational entropy plays a similar role in Al_2Sr.

As was the case for Al–Cu, we emphasize that this discrepancy between first-principles calculated energetics and observed stable crystal structures is unexpected. Hence, to verify the results, we have carefully performed additional calculations of Al_2Sr using VASP–PAW and FLAPW approaches as well as a gradient-corrected exchange correlation functional within the GGA. The VASP–PAW–LDA results confirm the VASP–LDA results showing that the *C*15 is lower in energy than $CeCu_2$-type for Al_2Sr. However, the VASP–GGA calculations predict the reverse order from VASP–LDA, giving the observed $CeCu_2$-type/*C*15 stability. Thus, because the GGA results are more consistent with the observed phase stability, one would like to conclude that the GGA simply provides a more accurate description of Al–Sr. As we will show below, calculations for other stoichiometries also point towards GGA as yielding more accurate energetics for this system. Nevertheless, an investigation of the vibrational entropies (via both LDA and GGA) of the $CeCu_2$ and *C*15 phases in Al_2Sr would certainly provide insight into this interesting structural competition.

We should note that this type of qualitative contrast between LDA and GGA predicted structural stability of intermetallics is exceedingly rare. Pure Fe provides the most well-known example of this dichotomy (with LDA incorrectly predicting a non-magnetic close-packed ground state, whereas GGA predicts the correct ferromagnetic bcc structure [55–58]), however, a recent study has shown that Fe_3Al also produces such a distinction [59]. In this case, though, LDA predicts the observed $D0_3$ phase, whereas GGA shows the $L1_2$ phase to be lower in energy. Both of these cases (Fe and Fe_3Al) are complicated by the fact that not only structural, but also magnetic effects come into play. Hence, to our knowledge, our results here provide the first-known case for a qualitative discrepancy between LDA and GGA

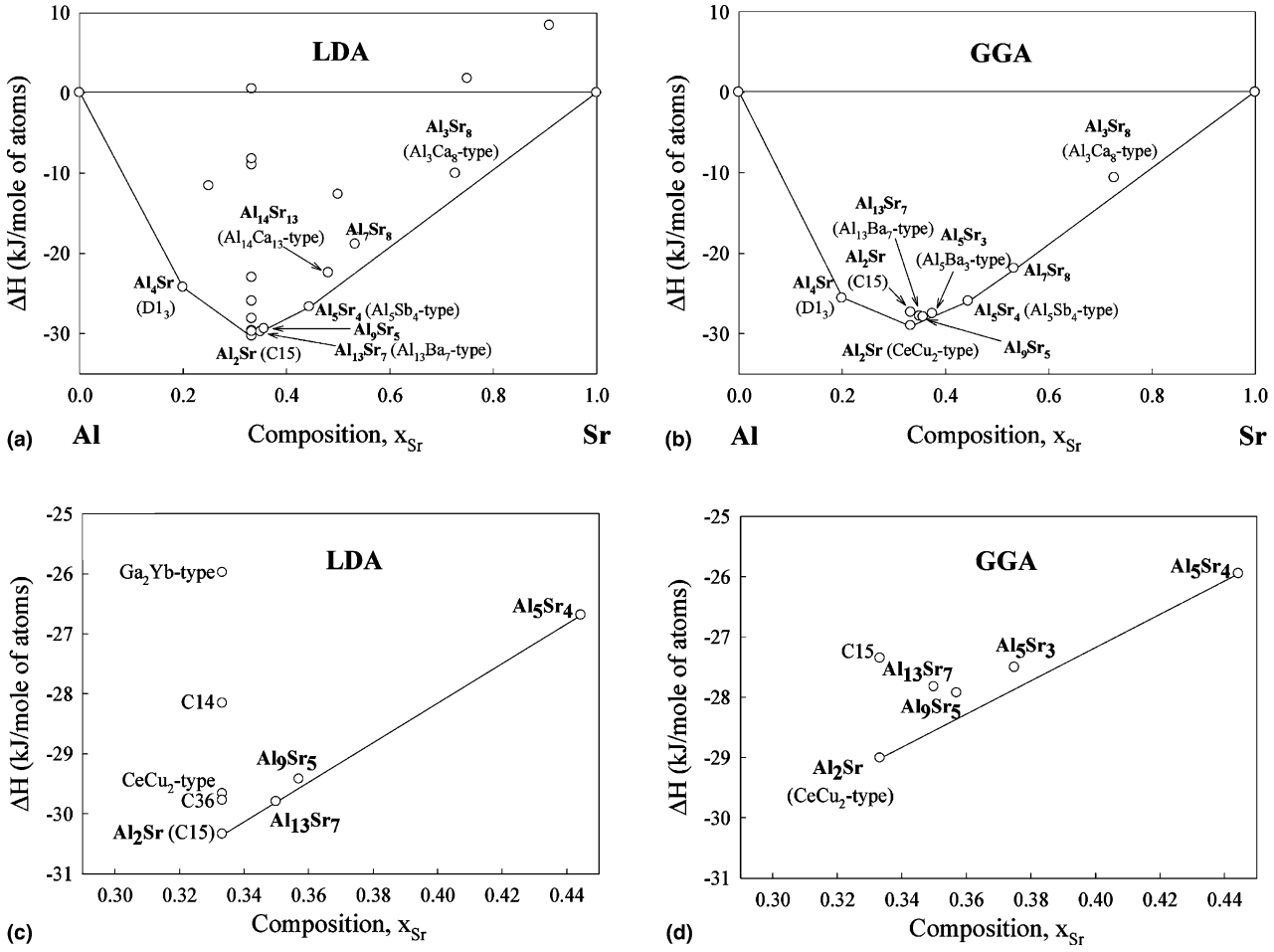

Fig. 1. First-principles VASP calculated formation enthalpies of Al–Sr in various ordered intermetallic structure types at 0 K. (a) LDA; (b) GGA; (c) and (d) are detailed views of the composition region near Al_2Sr stoichiometry.

structural stabilities for a non-magnetic intermetallic compound.

6.3. Near Al_2Sr stoichiometry: $Al_{13}Sr_7$ and Al_9Sr_5

There are reports of compounds near Al_2Sr stoichiometry, but slightly more Sr-rich: $Al_{13}Ba_7$ and Al_5Ba_3 are observed in the Al–Ba system and there has also been a report of an Al_9Sr_5 structure in Al–Sr. Our calculations of the energetics of these structures in Al–Sr show that they are very energetically competitive with the tie line connecting the Al_2Sr and more Sr-rich compounds. But, in both cases, our results demonstrate that there is not a clear energetic preference for these phases at $T = 0$ K. Again, entropic effects, especially vibrational, would be interesting to investigate the finite temperature stability (or lack of it) of these phases.

6.4. Near AlSr stoichiometry: Al_7Sr_8 and Al_5Sr_4

There are a rich variety of observed compounds near "AB" composition in the systems in Table 2. Al_7Sr_8 is observed as a stable phase in Al–Sr, at least at high temperatures [16]. The low temperature stability of this compound, however, is unknown. In the LDA calculation, the energy of Al_7Sr_8 falls significantly above the ground state hull of our calculations (Fig. 1). However, the GGA energy for Al_7Sr_8 is significantly lower and falls on the ground state hull. Thus, the GGA energetics again appears to be more consistent with experimental reports. It is noteworthy, however, that previous CALPHAD modeling of Al–Sr [23] has provided energetics that demonstrate an instability of Al_7Sr_8 as temperature is lowered, in agreement with the LDA results.

Interestingly, an Al_5Sr_4 (Al_5Sb_4-type) structure breaks the ground-state hull for both LDA and GGA. This phase has not been reported in Al–Sr (though it has in Al–Ba), and our results predict that there are new, as yet undiscovered, low-temperature ground states in Al–Sr near AlSr stoichiometry. Knowledge of the vibrational entropies would help sort out a more complete picture of the phase stability of all of the compounds that fall near the ground state tie-line between Al_2Sr and Sr: C15, $CeCu_2$, $Al_{13}Sr_7$, Al_9Sr_5, Al_5Sr_3, Al_5Sr_4, and Al_7Sr_8.

6.5. Sr-rich stoichiometries: Al_3Sr_8

It is interesting that of all the systems in Table 2, the Al-containing systems, Al–Sr and Al-Ba, are the only systems for which B-rich phases have not been reported. And, the existence of an Al_3Ca_8 Ca-rich compound in Al–Ca has only been discovered in the past few years [21,22]. The recent discoveries in Al–Ca, coupled with the unusual liquidus behavior for Sr-rich Al–Sr alloys (see below), indicate a likelihood that as yet undiscovered Sr-rich compound(s) exist in the Al–Sr phase diagram. Our calculations show that none of the Sr-rich compounds lie below the tie-line between Al_5Sr_4 and pure Sr. Therefore, our first-principles results do not predict any new $T = 0$ K Sr-rich ground states. However, the Al_3Sr_8 phase is competitive in energy, and we have included the Al_3Sr_8 phase nevertheless in our modeling as a temperature-stabilized phase (not a $T = 0$ K ground state). In a recent first-principles/CALPHAD study of Al–Ca, first-principles calculations show that the Al_3Ca_8 phase does indeed lie on the ground-state hull [60], in agreement with the recent discovery of this stable compound.

Our Al–Sr results demonstrate that new and unexpected results can be found by expanding the set of candidate structures beyond those observed in the system of interest. In many cases, it is suggested that the effects of vibrational entropy could play a significant role in the phase stability of this system, and therefore a future first-principles calculation of vibrational entropies in Al–Sr would be of interest. We also note that the GGA–PAW calculations are physically accurate and show consistently the best agreement with experimental observations. Therefore, in the CALPHAD optimization described below we use the GGA–PAW calculated energetics for all the compounds considered in this system.

7. Thermodynamic models

We next describe the thermodynamic models used in the CALPHAD description. There are two types of phases in the system, i.e., solution phases and intermetallic compounds described by sublattice models [24]. The solution phases are described with one sublattice, the intermetallic compounds with two. Due to the difficulties encountered in previous studies in accurately describing the Al–Sr energetics, we have contrasted two distinct thermodynamic evaluations for the liquid phase in this paper: the random solution and associate models. The associate model has been widely used to describe the thermodynamic properties of liquid alloys exhibiting short range order (SRO), using associates having a well-defined stoichiometric composition [25–27]. The liquid can be then described as a mixture of associates and the free atoms.

In many binary systems containing alkali earth metals, stoichiometric intermetallic compounds often form with melting temperatures much higher than those of the constitutive pure elements. Correspondingly, there is a deep minimum in the enthalpy of mixing in the liquid phase. When the random solution model is used for the liquid phase with the Redlich–Kister polynomial [61], it is found that higher-order interaction parameters in the liquid are typically needed to reproduce the liquidus around the high-melting temperature intermetallic compounds, and it often results in a less satisfactory liquidus at other compositions. The Al–Sr binary system is one of these systems with compounds (Al_4Sr and Al_2Sr) of very high melting temperatures compared to those of pure Al and Sr. A short-range ordering tendency in the liquid state in this system is likely as discussed by Sommer et al. [11] and Srikanth and Jacob [17]. Moreover, in recent experimental studies on the isoelectronic liquids, Al–Ca and Al–Ba [62,63], A_2B type short-range order was found. By analogy, it is reasonable to assume that short-range order also exists in liquid Al–Sr alloys and therefore an associate model is applicable in this system.

The associate model was used by Sommer et al. [11] and Srikanth and Jacob [17] in modeling the Al–Sr system, and in both cases, Al_2Sr was used as the associate. In the present study, Al_4Sr and Al_2Sr were chosen as the associates in the liquid Al–Sr solution. Here are the criteria commonly used to determine the compositions of associates:

(i) Negative enthalpies of mixing with a sharp change in slope near a stoichiometric composition.
(ii) In the solid state, a compound of the same stoichiometric composition exists.
(iii) The compound with the highest melting temperature corresponds to an associate with same composition in the liquid.

In the Al–Sr system, the enthalpies of mixing point to Al_2Sr as one of the associates and the Al_4Sr compound has the highest melting temperature in the system, indicating a tendency for the Al_4Sr associate in the liquid.

We next give detailed expressions for the Gibbs energy of each of the phases.

7.1. Solution phases: liquid, fcc, and bcc

7.1.1. Random solution model

The liquid phase in the random solution model and the fcc and bcc phases are treated with one sublattice model (Al, Sr), with the molar Gibbs energy expressed as

$$G_{\mathrm{m}}^{\Phi} = x_{\mathrm{Al}}{}^{0}G_{\mathrm{Al}}^{\Phi} + x_{\mathrm{Sr}}{}^{0}G_{\mathrm{Sr}}^{\Phi} + RT(x_{\mathrm{Al}}\ln x_{\mathrm{Al}} + x_{\mathrm{Sr}}\ln x_{\mathrm{Sr}}) + {}^{\mathrm{xs}}G_{\mathrm{m}}^{\Phi}, \quad (3)$$

where ${}^0G_i^{\Phi}$ is the molar Gibbs energy of the element i with the structure Φ, from [64]. ${}^{xS}G_m^{\Phi}$ is the excess Gibbs energy, expressed in Redlich–Kister polynomials [61],

$$ {}^{xS}G_m^{\Phi} = x_{Al}x_{Sr}\sum_{j=0}^{n} {}^jL_{Al,Sr}(x_{Al}-x_{Sr})^j, \tag{4} $$

where, ${}^jL_{Al,Sr}$ is the jth binary interaction parameter, ${}^jL = {}^jA + {}^jBT$. ${}^jA$ and ${}^jB$ are the model parameters to be evaluated.

7.1.2. Associate model

The liquid phase in the associate model is assumed to have four species (i.e., Al, Sr, Al_2Sr, and Al_4Sr). The Gibbs energy of the liquid is written as:

$$ \begin{aligned} G_m^L =& y_{Al}^0 G_{Al}^L + y_{Sr}^0 G_{Sr}^L + y_{Al_4Sr}^0 G_{Al_4Sr}^L + y_{Al_2Sr}^0 G_{Al_2Sr}^L \\ &+ RT(y_{Al}\ln y_{Al} + y_{Sr}\ln y_{Sr} + y_{Al_4Sr}\ln y_{Al_4Sr} \\ &+ y_{Al_2Sr}\ln y_{Al_2Sr}) + {}^{xs}G_m^L, \end{aligned} \tag{5} $$

where y represents the mole fractions of each species in the liquid. G_{Al}^L and G_{Sr}^L are the Gibbs energies of the pure Al and Sr liquid from [64], and $G_{Al_4Sr}^L$ and $G_{Al_2Sr}^L$ are the Gibbs energy of the associates Al_4Sr and Al_2Sr in the liquid phase. ${}^{xS}G_m^L$ is again the excess Gibbs energy and expressed as follows:

$$ \begin{aligned} {}^{xs}G_m^L =& y_{Al}y_{Sr}\sum_{j=0}^{n} {}^jL_{Al,Sr}^L(y_{Al}-y_{Sr})^j \\ &+ y_{Al}y_{Al_4Sr}\sum_{j=0}^{n} {}^jL_{Al,Al_4Sr}^L(y_{Al}-y_{Al_4Sr})^j \\ &+ y_{Al_4Sr}y_{Sr}\sum_{j=0}^{n} {}^jL_{Al_4Sr,Sr}^L(y_{Al_4Sr}-y_{Sr})^j \\ &+ y_{Al}y_{Al_2Sr}\sum_{j=0}^{n} {}^jL_{Al,Al_2Sr}^L(y_{Al}-y_{Al_2Sr})^j \\ &+ y_{Al_2Sr}y_{Sr}\sum_{j=0}^{n} {}^jL_{Al_2Sr,Sr}^L(y_{Al_2Sr}-y_{Sr})^j \\ &+ y_{Al_2Sr}y_{Al_4Sr}\sum_{j=0}^{n} {}^jL_{Al_2Sr,Al_4Sr}^L(y_{Al_2Sr}-y_{Al_4Sr})^j, \end{aligned} \tag{6} $$

where ${}^jL_{Al,Sr}^L$, ${}^jL_{Al,Al_4Sr}^L$, ${}^jL_{Al_4Sr,Sr}^L$, ${}^jL_{Al,Al_2Sr}^L$ ${}^jL_{Al_2Sr,Sr}^L$, and ${}^jL_{Al_4Sr,Al_2Sr}^L$ are the jth interaction parameters among the species Al, Sr, and the two associates Al_4Sr and Al_2Sr, ${}^jL = {}^jA + {}^jBT$. ${}^jA$ and ${}^jB$ are the model parameters to be evaluated.

7.2. Intermetallic phases

We consider four intermetallic compounds Al_4Sr, Al_2Sr, Al_7Sr_8, and Al_3Sr_8 in the Al–Sr system (see Table 1). They are modeled as stoichiometric compounds, and their Gibbs energy functions are written as:

$$ G_m^{Al_aSr_b} = a^0G_{Al}^{fcc} + b^0G_{Sr}^{fcc} + A^{Al_aSr_b} + B^{Al_aSr_b}T, \tag{7} $$

where ${}^0G_{Al}^{fcc}$ and ${}^0G_{Sr}^{fcc}$ are the molar Gibbs energies of the fcc Al and fcc Sr, respectively. $A^{Al_aSr_b}$ and $B^{Al_aSr_b}$ are the enthalpy and entropy of formation of the compound.

8. Optimization procedures and results

All model parameters were evaluated using the Parrot module [65] in Thermo-Calc [66]. This program takes a variety of experimental data simultaneously. It works by minimizing the error weighted and summed over each of the selected data. The weight is chosen and adjusted based upon the data uncertainties given in the original publications and upon the present authors' judgments by examining all experimental data concurrently. All thermodynamic calculations are carried out using Thermo-Calc. Our complete and self-consistent thermodynamic description for the Al–Sr binary system thus obtained is listed in Appendix A. The reference state of the Gibbs energy of individual phases is the Standard Element Reference (SER), i.e., the enthalpies of the pure elements in their stable states at 298.15 K and zero entropy at 0 K [64].

The optimization procedure starts with the liquid phase and its equilibria with the pure Al and Sr phases. The model parameters of the Al_4Sr phase were then evaluated because of the congruent melting of the phase and the extensive liquidus associated with the Al_4Sr phase. The thermodynamic parameters of the other phases were optimized one after another. Many iterations were necessary to reproduce all experimental and first-principles data. Subsequently, one final iteration was performed, optimizing all model parameters of all phases simultaneously including all experimental and first-principles data. Using this procedure, we obtained the model parameters given in Appendix A.

The calculated phase diagram using a random solution model for the liquid phase is shown in Fig. 2(a). Interaction parameters up to the second order, ${}^2L_{Al,Sr}^{liq}$, were used for the liquid. In the associate model, the Gibbs energies of formation of the Al_4Sr and Al_2Sr species in the liquid are calculated using two optimizing variables for each species. In addition, the interactions between each species (including the free atoms Al and Sr and the two associates Al_4Sr and Al_2Sr) can exist: ${}^0L_{Al,Sr}^{liq}$, ${}^0L_{Al,Al_4Sr}^{liq}$, ${}^0L_{Sr,Al_4Sr}^{liq}$, ${}^0L_{Al,Al_2Sr}^{liq}$, ${}^0L_{Sr,Al_2Sr}^{liq}$, and ${}^0L_{Al_4Sr,Al_2Sr}^{liq}$. Our results suggest that the two associates comprise a large amount of the liquid, and we only consider the interaction between Sr and Al_2Sr. The resulting phase diagrams from the associate model are shown in Figs. 3(a) and 4(a). A comparison of the calculated and experimental temperatures and Sr contents in a liquid phase at invariant equilibria are given in Table 4. For the concentration range less than 80 at.% Sr, the computed liquidus agrees well with the data from Closset et al. [15]. Small differences are found between the random solution model and the associate

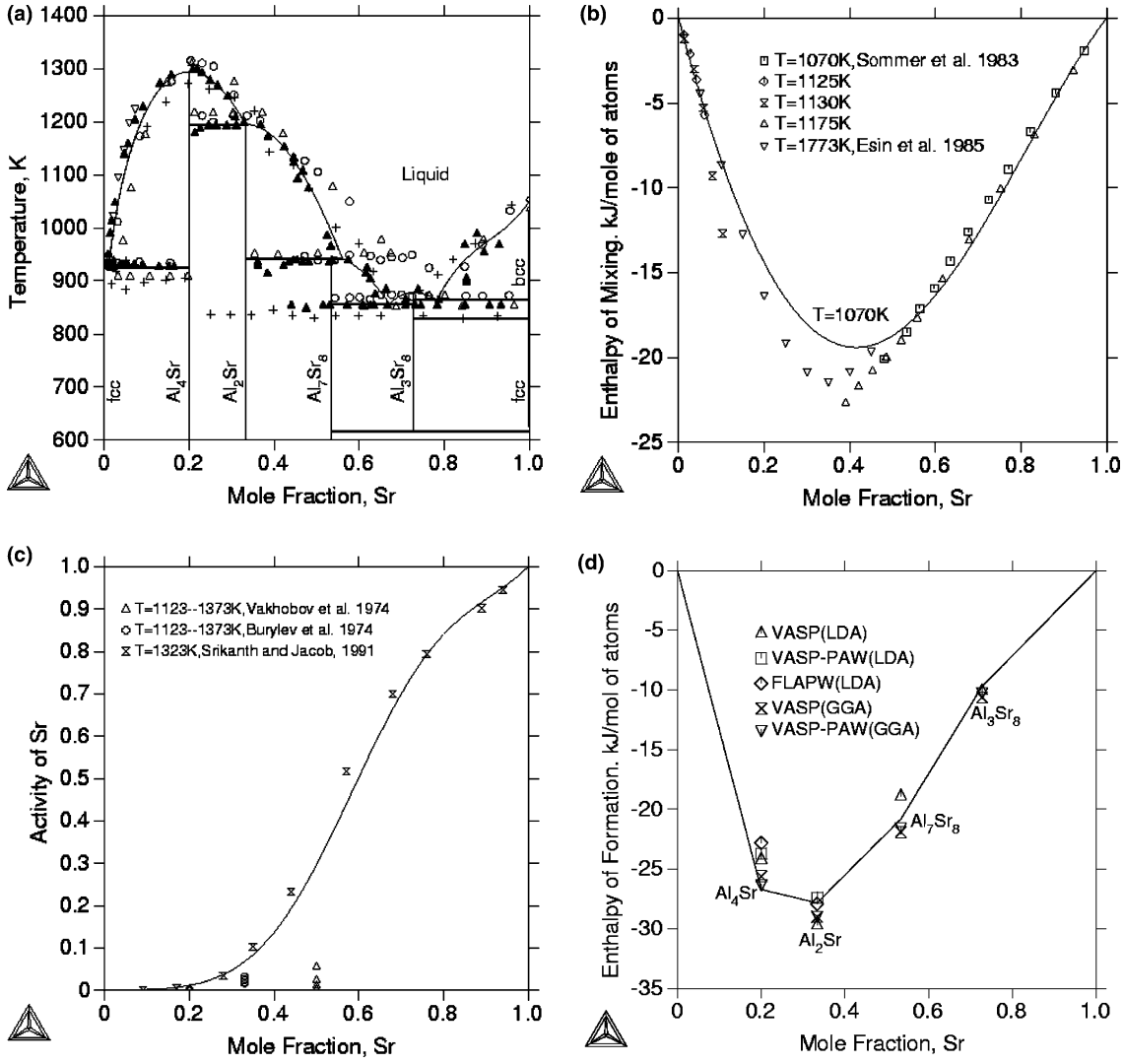

Fig. 2. The calculated results for the Al–Sr system using the random solution model and including the compound Al_3Sr_8: (a) the calculated phase diagram, compared with experimental data (+) by Vakhobov et al. [6], (○) by Bruzzone and Merlo [7], (△) by Vakhobov et al. [9], (⅄) by Hanna and Hellawell [10], (▲) by Closset et al. [15], and (▽) by Sato et al. [13]; (b) the enthalpy of mixing at 1070 K, (c) the activity of Sr in the liquid phase as a function of Sr concentration at 1323 K compared with experimental data of Srikanth and Jacob [17] at 1323 K, by Vakhobov et al. [6] at 1123–1373 K, and by Burylev et al. [5] at 1123–1373 K. The reference states are liquid Al and Sr at 1323 K; (d) the enthalpy of formation at 800 K as a function of the Sr concentration, compared with first-principles $T = 0$ K predictions. The reference states are Al and Sr fcc phases at 800 K.

model for the melting temperature of Al_4Sr and the liquidus around the Al_4Sr composition. A similar difference also exists in the calculated eutectic reactions involving Al_4Sr and Al_2Sr. The comparison shows the calculated phase diagram from the random solution model fits better to the experimental data from Closset et al. [15] than that from the associate model in the region between Al_4Sr and Al_2Sr composition.

The stability ranges of the Al_7Sr_8 and Al_3Sr_8 compounds have not been reported in the literature. Based on the GGA first-principles calculation results, Al_7Sr_8 is a stable $T = 0$ K compound, but Al_3Sr_8 is not. Thus, if Al_3Sr_8 is stable at high temperatures, it will decompose at lower temperatures. We have given this lower decomposition temperature (somewhat arbitrarily) a value of 650 ± 100 K. The Al_3Sr_8 compound has not been observed experimentally in the system; however, several experimental reports do point to a possible "fingerprint" for the stability of this phase: The liquidus around the Al_3Sr_8 composition is higher than the surrounding compositions. In spite of the rather close internal consistency between the calculated thermodynamic values (and phase diagram) and available experimental and first-principles-calculated thermochemical values (and experimentally determined phase equilibrium data), additional experiments in the Sr-rich region of the system would be desirable particularly with respect to the phases in equilibrium with the intermetallic phase Al_3Sr_8.

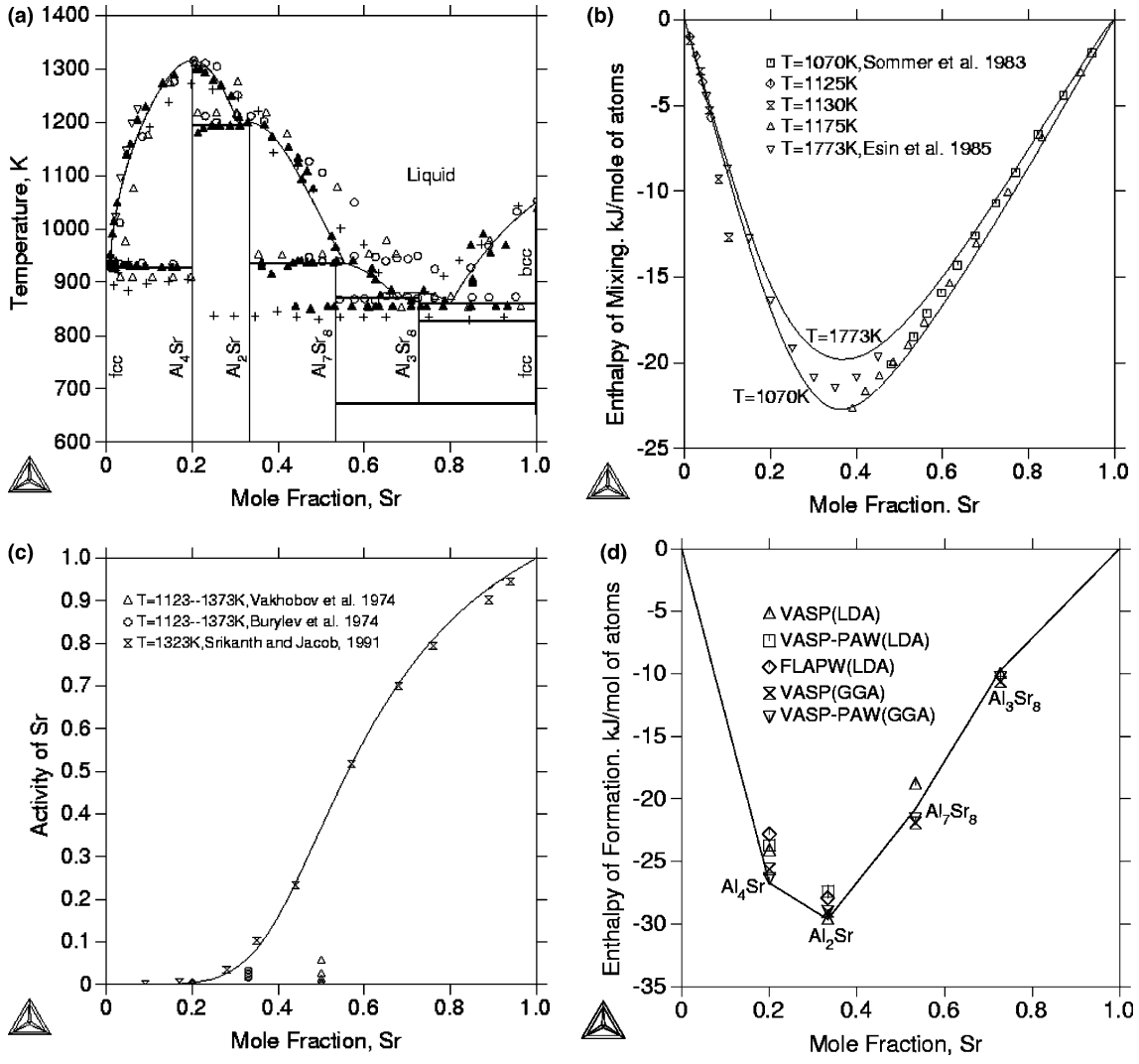

Fig. 3. The calculated results for the Al–Sr system using an associate model and including the compound Al_3Sr_8: (a) the calculated phase diagram, compared with experimental data (+) by Vakhobov et al. [6], (○) by Bruzzone and Merlo [7], (△) by Vakhobov et al. [9], (⅄) by Hanna and Hellawell [10], (▲) by Closset et al. [15], and (▽) by Sato et al. [13]; (b) the enthalpy of mixing at 1070 K, (c) the activity of Sr in the liquid phase as a function of Sr concentration at 1323 K compared with experimental data of Srikanth and Jacob [17] at 1323 K, by Vakhobov et al. [6] at 1123–1373 K, and by Burylev et al. [5] at 1123–1373 K. The reference states are liquid Al and Sr at 1323 K; (d) the enthalpy of formation at 800 K as a function of the Sr concentration, compared with first-principles $T = 0$ K predictions. The reference states are Al and Sr fcc phases at 800 K.

One might wonder why the Al_5Sr_4 compound was not included in the CALPHAD assessment despite its predicted stability according to first-principles calculations. The absence of this phase is simply due to the complete lack of experimental data for this phase; without further experimental information (or a first-principles prediction of the *entropy* of this and other phases), we simply cannot determine the phase stability of Al_5Sr_4 at elevated temperatures. Future experimental and/or first-principles work on this phase would therefore be of interest.

The enthalpy of mixing in the liquid from the random solution model, shown in Fig. 2(b), agrees reasonably well with experimental measurements at various temperatures. However, the liquid enthalpies from the associate model in Figs. 3(b) and 4(b) show a much better agreement with experiments. There is a very deep valley in the enthalpy of formation in the system with the minimum of the curve indicating strong interactions between the atoms in the liquid at compositions around the Al_2Sr phase. At 1070 K, the minimum point is at $x_{Sr} \approx 0.36$ and $\Delta H = -22.7$ kJ/mol, while at 1773 K it is at $x_{Sr} \approx 0.37$ and $\Delta H = -19.8$ kJ/mol when using the associate model. The temperature dependence of the enthalpy of mixing is due to the change of the amount of the associate in the liquid. On the other hand, in the random solution model, the enthalpy of mixing in the liquid phase is independent of temperature because the interaction parameter ${}^{i}L^{liq}_{Al,Sr}$ is represented by

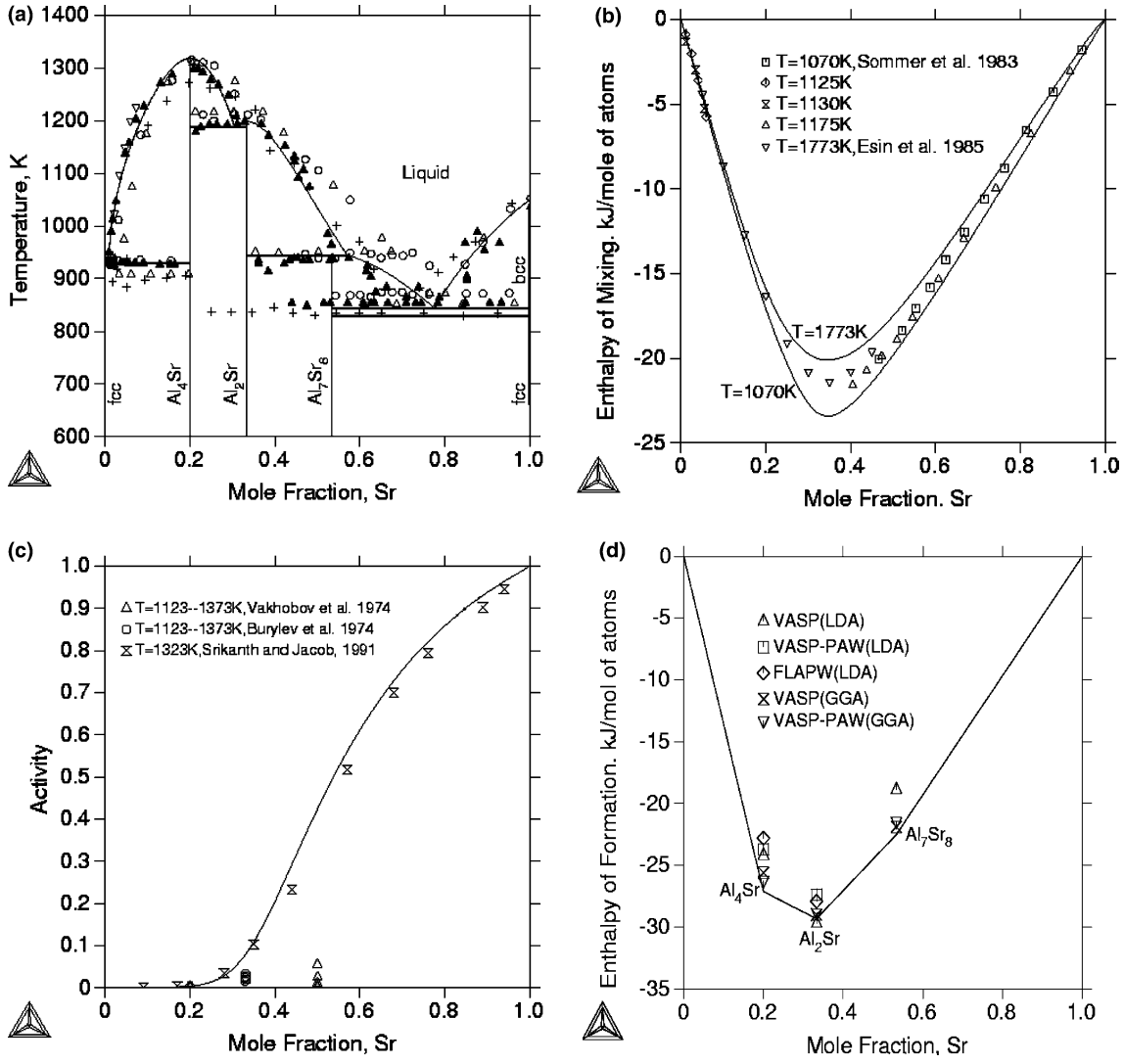

Fig. 4. The calculated results for the Al–Sr system using an associate model but without the compound Al_3Sr_8: (a) the calculated phase diagram, compared with experimental data (+) by Vakhobov et al. [6], (○) by Bruzzone and Merlo [7], (△) by Vakhobov et al. [9], (⅄) by Hanna and Hellawell [10], (▲) by Closset et al. [15], and (▽) by Sato et al. [13]; (b) the enthalpy of mixing at 1070 K, (c) the activity of Sr in the liquid phase as a function of Sr concentration at 1323 K compared with experimental data of Srikanth and Jacob [17] at 1323 K, by Vakhobov et al. [6] at 1123–1373 K, and by Burylev et al. [5] at 1123–1373 K. The reference states are liquid Al and Sr at 1323 K; (d) the enthalpy of formation at 800 K as a function of the Sr concentration, compared with first-principles $T = 0$ K predictions. The reference states are Al and Sr fcc phases at 800 K.

${}^{j}A + {}^{j}BT$. The minimum point is at $x_{Sr} \approx 0.41$ and $\Delta H = -19.4$ kJ/mol when using the random solution model. Figs. 2(c), 3(c), and 4(c) show the activities of Sr in the liquid at 1323 K with good agreement between the experimental data and calculation results in each case. Similarly to the above, the results from the associate model fit the experimental results better than that from the random solution model.

Figs. 2(d), 3(d), and 4(d) present the enthalpy of formation of the present modeling at 800 K with the symbols being the $T = 0$ K first-principles calculation results. The first-principles calculation results of the enthalpies of formation for the four compounds using GGA–PAW approach are treated as the experimental information of those compounds at 298 K. The agreement between the first-principles energetics and the final calculated values indicates that our modeling retains accurate, physically based energetics for the solid-state portion of the phase diagram. One should note that the enthalpy of formation in Figs. 2(d) and 3(d) does not form a convex shape with respect to the composition, although the free energy must be convex. The shape of the enthalpy curves in Figs. 2(d) and 3(d) demonstrates that, consistent with the first-principles calculations, Al_3Sr_8 is not stable at low temperatures when the entropy contribution to the Gibbs energy is less significant and the phase stability is predominantly controlled by the enthalpy of formation of the compounds.

Table 4
Invariant equilibria in the A1–Sr binary system (composition in the liquid phase)

Reaction		Liquid $= Al(fcc) + Al_4Sr$	Liquid $= Al_4Sr$	Liquid $= Al_4Sr + Al_2Sr$	Liquid $= Al_2Sr$	Liquid $+ Al_2Sr = Al_7Sr_8$
Reaction type		Eutectic	Congruent	Eutectic	Congruent	Peritectic
Experimental data		903 ± 5 K, 3.2 at.% Sr[5]; 903 K, 3.3 at.% Sr [6,8]; 908 K, 3.2 at.% Sr [9]; 926 K, 1.3 at.% Sr [10]; 927 K, 0.85 at.% Sr [13]; 927 K, 0.75 at.% Sr [15]	1273 ± 20 K [5], 1273 K [6,8]; 1313 K [7,9], 1298 K [15]; 20 at.% Sr	/	/	/
Random solution model with Al_3Sr_8	T (K)	925	1295	1195	1195	941
	at.% Sr	1.12	20.00	33.25	33.33	56.06
Associate model with Al_3Sr_8	T (K)	928	1316	1194	1199	936
	at.% Sr	0.75	20.00	30.90	33.33	55.50
Associate model without Al_3Sr_8	T (K)	929	1319	1188	1199	942
	at.% Sr	0.68	20.00	30.48	33.33	57.09

The amount of each species in the liquid calculated from associate model is shown in Fig. 5. It is found that about 65% of the species in the liquid is Al_2Sr at compositions around 33 at.% Sr and about 16% of the species in the liquid is Al_4Sr at compositions around 20 at.% Sr at 1300 K, which is around the melting temperature of Al_4Sr. It seems there is a large amount of short-range order in the liquid at low temperature, which may be the reason for the higher accuracy of the calculated enthalpy of mixing in the liquid phase from the associate model. To elucidate the extent of the short-range order in these alloys, a future first-principles simulation of liquid Al–Sr alloys would be of interest.

All the above comparisons between the random solution model and the associate model shows the random solution model yields better agreement with the experimental phase equilibrium data in the region between Al_4Sr and Al_2Sr, while the associate model gives better agreement with experimental thermodynamic data. The thermodynamic description of the associate model is thus recommended, because it contains a more solid physical foundation for its description of the thermodynamic properties.

9. Summary

Motivated by the lack of accurate solid and/or liquid energetics in previous Al–Sr thermodynamic assessments, we have undertaken a new investigation of the Al–Sr system by combining first-principles density-functional calculations, experimental thermodynamic and phase stability data, and a CALPHAD modeling

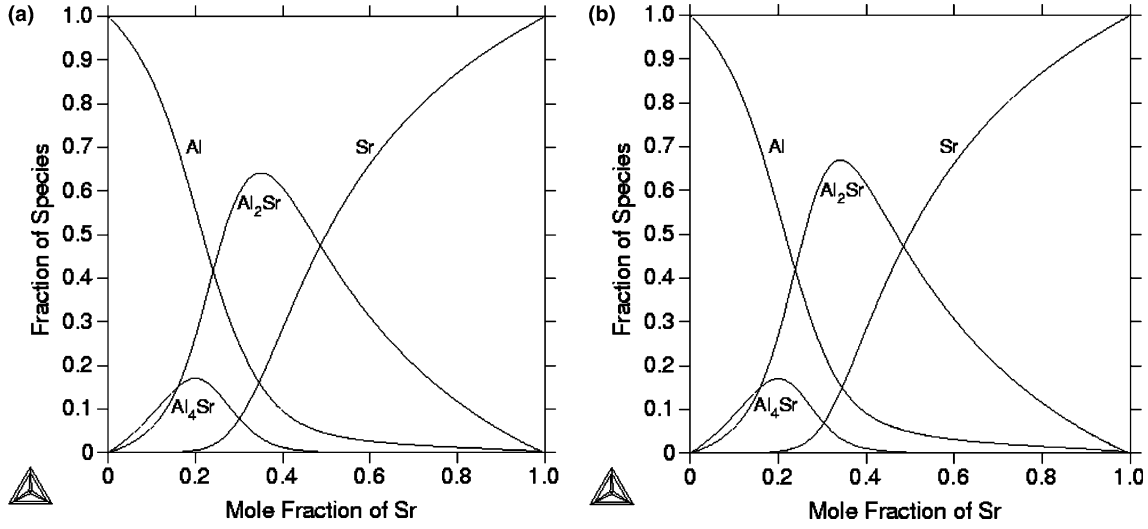

Fig. 5. Mole fraction of each species as a function of the Sr concentration in the liquid phase, calculated using the associate model for the liquid phase at 1300 K: (a) with Al_3Sr_8 and (b) without Al_3Sr_8.

approach. Via first-principles methods, we have investigated the $T = 0$ K energetics of not only the reported ground state compounds in Al–Sr, but also of a many other possible crystal structures observed in isoelectronic A–B alloy systems (A = Al,Ga,In; B = Ca,Sr,Ba). From this pool of candidate crystal structures, we find some surprising results: (i) There is a qualitative discrepancy between the LDA- and GGA-predicted $T = 0$ K stabilities of the $CeCu_2$-type and $C15$ phases at Al_2Sr stoichiometry. To our knowledge, this is the first known qualitative discrepancy of this type found for a non-magnetic, metallic system. (ii) We predict the existence of new phases in Al–Sr, stable at least at low temperatures: an as-yet-unreported Al_5Sr_4 compound – observed in Al–Ba – is found to be on the first-principles-predicted $T = 0$ K ground state hull (for both LDA and GGA). (iii) In contrast, an Al_3Sr_8 phase, isostructural with the recently discovered Al_3Ca_8 compound, is predicted to lie above the ground state hull and is not a $T = 0$ K ground state. However, the observed behavior of the liquidus for Sr-rich alloys suggests the possible existence of this (or some other) phase at high temperatures.

By combining these first-principles energetics with a critical review of the available experimental thermochemical and phase diagram data, we have produced a new CALPHAD thermodynamic description of Al–Sr. Our description possesses liquid enthalpies that compare favorably with the most accurate experimental data and solid-state enthalpies that agree well with first-principles calculations. We have tested a set of three different models for the liquid phase: (1) an associate model without the phase Al_3Sr_8, (2) a random solution model including Al_3Sr_8, and (3) an associate model including Al_3Sr_8. We find that the random solution model yields better agreement with the experimental phase equilibrium data in the region between Al_4Sr and Al_2Sr composition, while the associate model gives better agreement with experimental thermodynamic data.

Acknowledgements

This work is supported by the NSF CAREER Award under the Grant DMR-9983532. The Thermo-Calc program is licensed from The Foundation for Computational Thermodynamics, Stockholm, Sweden. Y.A.C. wishes to thank Zhu Jun for repeating many of calculations in terms of phase diagrams and thermodynamic values and the National Science Foundation (Grant No. NSF-DMR-03-09468) and Wisconsin Distinguished Professorship for financial support.

Appendix A

Thermodynamic parameters for the Al–Sr system in SI units (parameters not listed are all zero)

	Phase	Sublattice model	Evaluated description
Random solution model	Liquid	(Al,Sr)	${}^0L^{\mathrm{liq}}_{\mathrm{Al,Sr}} = -74,839 + 23.686T$
			${}^1L^{\mathrm{liq}}_{\mathrm{Al,Sr}} = -31,790 + 8.549T$
			${}^2L^{\mathrm{liq}}_{\mathrm{Al,Sr}} = 10,683 - 4.130T$
	Al_4Sr	$(Al)_{4/5}(Sr)_{1/5}$	${}^0G^{\mathrm{Al_4Sr}}_{\mathrm{m}} = 4/5\,{}^0G^{\mathrm{fcc}}_{\mathrm{Al}} + 1/5\,{}^0G^{\mathrm{fcc}}_{\mathrm{Sr}} - 26,686 + 6.846T$
	Al_2Sr	$(Al)_{2/3}(Sr)_{1/3}$	${}^0G^{\mathrm{Al_2Sr}}_{\mathrm{m}} = 2/3\,{}^0G^{\mathrm{fcc}}_{\mathrm{Al}} + 1/3\,{}^0G^{\mathrm{fcc}}_{\mathrm{Sr}} - 27,822 + 6.107T$
	Al_7Sr_8	$(Al)_{7/15}(Sr)_{8/15}$	${}^0G^{\mathrm{Al_7Sr_8}}_{\mathrm{m}} = 7/15\,{}^0G^{\mathrm{fcc}}_{\mathrm{Al}} + 8/15\,{}^0G^{\mathrm{fcc}}_{\mathrm{Sr}} - 20,813 + 3.150T$
	Al_3Sr_8	$(Al)_{3/11}(Sr)_{8/11}$	${}^0G^{\mathrm{Al_3Sr_8}}_{\mathrm{m}} = 3/11\,{}^0G^{\mathrm{fcc}}_{\mathrm{Al}} + 8/11\,{}^0G^{\mathrm{fcc}}_{\mathrm{Sr}} - 9708 - 2.150T$
Associate model with Al_3Sr_8	Liquid	(Al,Sr,Al_4Sr,Al_2Sr)	${}^0L^{\mathrm{liq}}_{\mathrm{Sr,Al_2Sr}} = -15,221$
			${}^0G^{\mathrm{Al_4Sr}}_{\mathrm{m}} = 4\,{}^0G^{\mathrm{liq}}_{\mathrm{Al}} + {}^0G^{\mathrm{liq}}_{\mathrm{Sr}} - 97,696 + 24.084T$
			${}^0G^{\mathrm{Al_2Sr}}_{\mathrm{m}} = 2\,{}^0G^{\mathrm{liq}}_{\mathrm{Al}} + {}^0G^{\mathrm{liq}}_{\mathrm{Sr}} - 75,525 + 13.055T$
	Al_4Sr	$(Al)_{4/5}(Sr)_{1/5}$	${}^0G^{\mathrm{Al_4Sr}}_{\mathrm{m}} = 4/5\,{}^0G^{\mathrm{fcc}}_{\mathrm{Al}} + 1/5\,{}^0G^{\mathrm{fcc}}_{\mathrm{Sr}} - 26,701 + 4.118T$
	Al_2Sr	$(Al)_{2/3}(Sr)_{1/3}$	${}^0G^{\mathrm{Al_2Sr}}_{\mathrm{m}} = 2/3\,{}^0G^{\mathrm{fcc}}_{\mathrm{Al}} + 1/3\,{}^0G^{\mathrm{fcc}}_{\mathrm{Sr}} - 29,610 + 4.762T$
	Al_7Sr_8	$(Al)_{7/15}(Sr)_{8/15}$	${}^0G^{\mathrm{Al_7Sr_8}}_{\mathrm{m}} = 7/15\,{}^0G^{\mathrm{fcc}}_{\mathrm{Al}} + 8/15\,{}^0G^{\mathrm{fcc}}_{\mathrm{Sr}} - 20,789 + 1.556T$
	Al_3Sr_8	$(Al)_{3/11}(Sr)_{8/11}$	${}^0G^{\mathrm{Al_3Sr_8}}_{\mathrm{m}} = 3/11\,{}^0G^{\mathrm{fcc}}_{\mathrm{Al}} + 8/11\,{}^0G^{\mathrm{fcc}}_{\mathrm{Sr}} - 9716 - 2.704T$
Associate model without Al_3Sr_8	Liquid	(Al,Sr,Al_4Sr,Al_2Sr)	${}^0L^{\mathrm{liq}}_{\mathrm{Sr,Al_2Sr}} = -8435$
			${}^0G^{\mathrm{Al_4Sr}}_{\mathrm{m}} = 4\,{}^0G^{\mathrm{liq}}_{\mathrm{Al}} + {}^0G^{\mathrm{liq}}_{\mathrm{Sr}} - 96,622 + 22.274T$
			${}^0G^{\mathrm{Al_2Sr}}_{\mathrm{m}} = 2\,{}^0G^{\mathrm{liq}}_{\mathrm{Al}} + {}^0G^{\mathrm{liq}}_{\mathrm{Sr}} - 77,919 + 13.842T$
	Al_4Sr	$(Al)_{4/5}(Sr)_{1/5}$	${}^0G^{\mathrm{Al_4Sr}}_{\mathrm{m}} = 4/5\,{}^0G^{\mathrm{fcc}}_{\mathrm{Al}} + 1/5\,{}^0G^{\mathrm{fcc}}_{\mathrm{Sr}} - 27,122 + 4.411T$
	Al_2Sr	$(Al)_{2/3}(Sr)_{1/3}$	${}^0G^{\mathrm{Al_2Sr}}_{\mathrm{m}} = 2/3\,{}^0G^{\mathrm{fcc}}_{\mathrm{Al}} + 1/3\,{}^0G^{\mathrm{fcc}}_{\mathrm{Sr}} - 29,301 + 4.340T$
	Al_7Sr_8	$(Al)_{7/15}(Sr)_{8/15}$	${}^0G^{\mathrm{Al_7Sr_8}}_{\mathrm{m}} = 7/15\,{}^0G^{\mathrm{fcc}}_{\mathrm{Al}} + 8/15\,{}^0G^{\mathrm{fcc}}_{\mathrm{Sr}} - 22,516 - 3.807T$

References

[1] Closset B, Gruzleski JE. Structure and properties of hypoeutectic Al–Si–Mg alloys modified with pure strontium. Metal Trans A 1982;13A:945–51.

[2] Hanna MD, Lu SZ, Hellawell A. Modification in the aluminum silicon system. Metal Trans A 1984;15A:459–69.

[3] Baril E, Labelle P, Pekguleryuz MO. Elevated temperature Mg–Al–Sr: creep resistance, mechanical properties, and microstructure. Jom-J Min Met Mater Sci 2003;55:A34–9.

[4] Nowotony H, Wesenberg H. Investigation of the aluminum–strontium system. Z Metalkd 1939;31:363–4.

[5] Burylev BP, Vakhobov AV, Dzhuraev TD. Thermodynamic activities of the components in alloys of aluminum with barium and strontium. Zh Fiz Khim 1974;48:1377–80.

[6] Vakhobov AV, Dzhuraev TD, Vigdorovich VN. Study of the vapor pressure over alloys of the aluminum–strontium system. Zh Fiz Khim 1974;48:2204–7.

[7] Bruzzone G, Merlo F. The strontium–aluminum and barium–aluminum systems. J Less-Common Met 1975;39:1–6.

[8] Vakhobov AV, Dzhuraev TD, Bardin VA, Zademidko GA. Constitution diagrams for the aluminum–strontium and lead–strontium systems. Izv Akad Nauk SSSR, Met 1975:194–7.

[9] Vakhobov AV, Eshonov KK, Dzhurayev TD. The Al–Sr–Nd phase diagram (Translation). Russ Metall 1979:167–72.

[10] Hanna MD, Hellawell A. Modification of Al–Si microstructure – the Al–Si–Sr phase diagram from 0 to 20 wt% silicon and 0–5.0 wt% strontium, alloy phase diagrams. Boston, MA: Elsevier; 1982. pp. 411–416.

[11] Sommer F, Lee JJ, Predel B. Thermodynamic investigations of liquid aluminum–calcium, aluminum–strontium, magnesium–nickel and calcium–nickel alloys. Z Metalkd 1983; 74:100–4.

[12] Kharif YL, Kovtunenko PV, Maier AA, Avetisov IH, Beebyakin MM. Thermodynamic calculation of the temperature-composition diagram and the Gibbs standard energy of compounds in the Ba–Al, Sr–Al and Ca–Al systems. Izv Akad Nauk SSSR, Neorg Mat 1984;20:1372–7.

[13] Sato E, Kono N, Sato I, Watanabe H. Study on the phase diagram of Al–Si–Sr ternary alloy system. J Jpn Inst Light Met 1985;35:71–8.

[14] Esin YO, Litovskii VV, Demin SE, Petrushevskii MS. Enthalpies of formation of aluminum–strontium and barium–silicon melts (Translation). Russ J Phys Chem 1985; 59:446–7.

[15] Closset B, Dugas H, Pekguleryuz M, Gruzleski JE. The aluminum–strontium phase diagram. Metal Trans 1986;17A:1250–3.

[16] Alcock CB, Itkin VP. The Al–Sr (aluminum–strontium) system. Bull Alloy Phase Diag 1989;10:624–30.

[17] Srikanth S, Jacob KT. Thermodynamics of aluminum–strontium alloys. Z Metalkd (Germany) 1991;82:675–83.

[18] Korc B, Panek Z, Fitzner K. Activity of strontium in Al–Sr liquid dilute solutions. Aluminium (Germany) 1992;68:784–6.

[19] Chartrand P, Pelton AD. Critical evaluation and optimization of the thermodynamic properties and phase diagrams of the Al–Mg, Al–Sr, Mg–Sr, and Al–Mg–Sr systems. J Phase Equilibr 1994;15:591–605.

[20] Wolverton C, Yan XY, Vijayaraghavan R, Ozolins V. Incorporating first-principles energetics in computational thermodynamics approaches. Acta Mater 2002;50:2187–97.

[21] Huang BQ, Corbett JD. Two new binary calcium–aluminum compounds: $Ca_{13}Al_{14}$, with a novel two-dimensional aluminum network, and Ca_8Al_3, an Fe_3Al-type analogue. Inorg Chem 1998;37:5827–33.

[22] Kevorkov D, Schmid-Fetzer R. The Al–Ca system, part 1: experimental investigation of phase equilibria and crystal structures. Z Metalkd 2001;92:946–52.

[23] Wang C, Jin Z, Du Y. Thermodynamic modeling of the Al–Sr system. J Alloy Compd 2003;358:288–93.

[24] Sundman B, Agren J. A regular solution model for phases with several components and sublattices, suitable for computer applications. J Phys Chem Solids 1981;42:297–301.

[25] Krull HG, Singh RN, Sommer F. Generalised association model. Z Metalkd 2000;91:356–65.

[26] Sommer F. Association model for the description of the thermodynamic functions of liquid alloys. I. Basic concepts. Z Metalkd 1982;73:72–6.

[27] Sommer F. Association model for the description of thermodynamic functions of liquid alloys. II. Numerical treatment and results. Z Metallkd 1982;73:77–86.

[28] Closset B, Dugas H, Pekguleryuz M, Gruzleski JE. The aluminum–strontium phase-diagram. Metal Trans A 1986;17: 1250–3.

[29] Kresse G, Hafner J. Abinitio molecular-dynamics for liquid-metals. Phys Rev B 1993;47:558–61.

[30] Kresse G. Thesis, Technische Universitat, Wien; 1993.

[31] Kresse G, Furthmuller J. Efficient iterative schemes for ab initio total-energy calculations using a plane-wave basis set. Phys Rev B 1996;54:11169–86.

[32] Kresse G, Furthmuller J. Efficiency of ab initio total energy calculations for metals and semiconductors using a plane-wave basis set. Comput Mater Sci 1996;6:15–50.

[33] Vanderbilt D. Soft self-consistent pseudopotentials in a generalized eigenvalue formalism. Phys Rev B 1990;41:7892–5.

[34] Kresse G, Hafner J. Norm-conserving and ultrasoft pseudopotentials for first-row and transition-elements. J Phys 1994;6:8245–57.

[35] Ceperly DM, Alder BJ. Ground state of the electron gas by a stochastic method. Phys Rev Lett 1980;45:566–9.

[36] Perdew JP, Zunger A. Self-interaction correction to density-functional approximations for many-electron systems. Phys Rev B 1981;23:5048–79.

[37] Wei SH, Krakauer H. Local-density-functional calculation of the pressure-induced metallization of BaSe and BaTe. Phys Rev Lett 1985;55:1200–3.

[38] Singh DJ. Planewaves, pseudopotentials, and the LAPW method. Boston: Kluwer; 1994.

[39] Monkhorst HJ, Pack JD. Special points for brillouin-zone integrations. Phys Rev B 1976;13:5188–92.

[40] Maddox J. Crystals from 1st principles. Nature 1988;335:201–201.

[41] Sanchez JM, Ducastelle F, Gratias D. Generalized cluster description of multicomponent systems. Physica A 1984;128: 334–50.

[42] de Fontaine D. Cluster approach to order–disorder transformations in alloys. Solid State Phys 1994;47:33–176.

[43] Zunger A. First-principles statistical mechanics of semiconductor alloys and intermetallic compounds. In: Turchi PEA, Gonis A, editors. Statics and dynamics of alloy phase transformations. New York: Plenum; 1994. p. 361–419.

[44] Ozolins V, Wolverton C, Zunger A. Cu–Au, Ag–Au, Cu–Ag, and Ni–Au intermetallics: first-principles study of temperature-composition phase diagrams and structures. Phys Rev B 1998;57:6427–43.

[45] Wolverton C, Ceder G, de Fontaine D, Dreysse H. Ab Initio determination of structural stability in Fcc-based transition-metal alloys. Phys Rev B 1993;48:726–47.

[46] Wolverton C, Zunger A. First-principles prediction of vacancy order–disorder and intercalation battery voltages in LixCoO2. Phys Rev Lett 1998;81:606–9.

[47] Van der Ven A, Aydinol MK, Ceder G. First-principles evidence for stage ordering in LixCoO2. J Electrochem Soc 1998;145:2149–55.

[48] Wolverton C, Ozolins V, Zunger A. First-principles theory of short-range order in size-mismatched metal alloys: Cu–Au, Cu–Ag, and Ni–Au. Phys Rev B 1998; 57:4332–48.

[49] Wolverton C, Ozolins V, Zunger A. Short-range-order types in binary alloys: a reflection of coherent phase stability. J Phys 2000;12:2749–68.
[50] Asta M, Defontaine D, Vanschilfgaarde M. First principles study of phase-stability of Ti–Al intermetallic compounds. J Mater Res 1993;8:2554–68.
[51] Lu ZW, Wei SH, Zunger A, Frotapessoa S, Ferreira LG. First principles statistical-mechanics of structural stability of intermetallic compounds. Phys Rev B 1991;44:512–44.
[52] Wolverton C. First-principles prediction of equilibrium precipitate shapes in Al–Cu alloys. Philos Mag Lett 1999;79:683–90.
[53] Zunger A, Wei SH, Ferreira LG, Bernard JE. Special quasirandom structures. Phys Rev Lett 1990;65:353–6.
[54] Wolverton C, Ozolins V. Entropically favored ordering: the metallurgy of Al2Cu revisited. Phys Rev Lett 2001;86:5518–21.
[55] Wang CS, Klein BM, Krakauer H. Theory of magnetic and structural ordering in iron. Phys Rev Lett 1985;54:1852–5.
[56] Singh DJ, Pickett WE, Krakauer H. Gradient-corrected density functionals – full-potential calculations for iron. Phys Rev B 1991;43:11628–34.
[57] Amador C, Lambrecht WRL, Segall B. Application of generalized gradient-corrected density functionals to iron. Phys Rev B 1992;46:1870–3.
[58] Haglund J. Fixed-spin-moment calculations on bcc and fcc iron using the generalized gradient approximation. Phys Rev B 1993;47:566–9.
[59] Lechermann F, Welsch F, Elsasser C, Ederer C, Fahnle M, Sanchez JM, Meyer B. Density-functional study of Fe3Al: LSDA versus GGA. Phys Rev B 2002;65, art. 132104.
[60] Ozturk K, Zhong Y, Chen L-Q, Wolverton C, Sofo JO, Liu Z-K. Linking first-principles energetics to CALPHAD: an application to thermodynamic modeling of Al–Ca binary system. Metal Mater Trans A 2003.
[61] Redlich AMO, Kister AT. Algebraic representations of thermodynamic properties and the classification of solutions. Ind Eng Chem 1948;40:345–8.
[62] You D, Schnyders HS, VanZytveld JB. Chemical short-range order and the Meyer–Neldel rule for liquid alloys: AlCa and GaAlCa. J Phys 1997;9:1407–15.
[63] Zuo D, Vos T, Nymeyer H, Reynolds L, Schnyders HS, VanZytveld JB. Electronic properties of the liquid alloys AlCa and AlBa. J Non-Cryst Solids 1996;207:328–31.
[64] Dinsdale AT. SGTE data for pure elements. CALPHAD 1991;15:317–425.
[65] Jansson B. Evaluation of parameters in thermochemical models using different types of experimental data simultaneously. Trita-Mac-0234, Royal Institute of Technology, Stockholm, Sweden; 1984.
[66] Andersson JO, Helander T, Hoglund LH, Shi PF, Sundman B. Thermo-Calc & DICTRA, computational tools for materials science. CALPHAD 2002;26:273–312.
[67] King HW. Cystal structures of the elements at 25 °C. Bull Alloy Phase Diagr 1981;2:401–2.
[68] Manyako NB, Zarechnyuk OS, Yanson TI. Crystal structure of Sr_5Al_9. Sov Phys Crystallogr 1987;32:196–9.
[69] Fornasini ML. Structures of Ba8Ga7, Sr8Ga7 and Sr8Al7. Acta Crystallogr, Sect C 1983;39:943–6.
[70] King HW. Temperature dependant allotropic sturctrues of the elements. Bull Alloy Phase Diagr 1982;3:275–6.